

See discussions, stats, and author profiles for this publication at: <https://www.researchgate.net/publication/280967074>

Optimization of a Stable Linker Involved DEVD Peptide–Doxorubicin Conjugate That Is Activated upon Radiation-Induced Caspase-3-Mediated Apoptosis

ARTICLE *in* JOURNAL OF MEDICINAL CHEMISTRY · AUGUST 2015

Impact Factor: 5.45 · DOI: 10.1021/acs.jmedchem.5b00420 · Source: PubMed

READS

18

7 AUTHORS, INCLUDING:



[Seung Woo Chung](#)

Seoul National University

20 PUBLICATIONS 116 CITATIONS

[SEE PROFILE](#)



[Sokwon Kim](#)

University of Ulsan

470 PUBLICATIONS 11,659 CITATIONS

[SEE PROFILE](#)

Optimization of a Stable Linker Involved DEVD Peptide-Doxorubicin Conjugate That Is Activated upon Radiation-Induced Caspase-3-Mediated Apoptosis

Seung Woo Chung,[†] Beom Suk Lee,^{‡,§} Jeong uk Choi,[†] Seong Who Kim,[⊥] In-San Kim,[§] Sang Yoon Kim,^{*,‡,§} and Youngro Byun^{*,†,||}

[†]Research Institute of Pharmaceutical Sciences, College of Pharmacy, Seoul National University, 151-742 Seoul, South Korea

[‡]Department of Otolaryngology, Asan Medical Center, University of Ulsan College of Medicine, 138-736 Seoul, South Korea

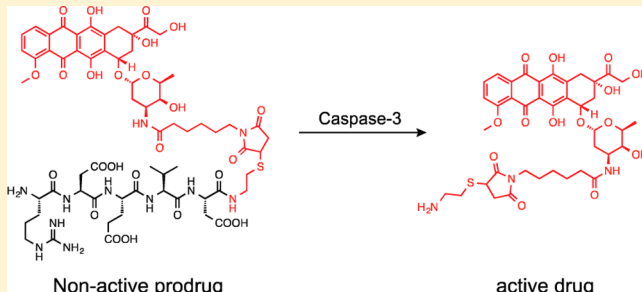
[§]Biomedical Research Institute, Korea Institute of Science and Technology, 136-791 Seoul, South Korea

^{||}Department of Molecular Medicine and Biopharmaceutical Sciences, Graduate School of Convergent Science and Technology, Seoul National University, 151-742 Seoul, South Korea

[⊥]Department of Biochemistry and Molecular Biology, Asan Medical Center, University of Ulsan College of Medicine, 138-736 Seoul, South Korea

Supporting Information

ABSTRACT: The current study demonstrates the process of selecting an optimal structure for a caspase-3-cleavable doxorubicin prodrug that could be synthesized by simple chemistry in high yields. The prodrug was intended to activate in the presence of caspase-3, whose expression can be exogenously regulated by inducing apoptosis with radiation therapy at a specific site of interest. For this purpose, doxorubicin was conjugated with a DEVD peptide via a heterobifunctional linker. Since the active form of the prodrug comprises the linker besides doxorubicin, we tested several different linkers and selected EMCS based on the examination of its *in vitro* biological activities. Consequently, DEVD-cysteamide-EMCS-doxorubicin was synthesized as the final compound. According to the various *in vitro* and *in vivo* studies, the synthesized prodrug was highly selective for tumors when coupled with radiation therapy, with the added benefit of ease of production.



INTRODUCTION

Despite the emergence of targeted therapy in modern cancer treatment, doxorubicin is still widely used for the treatment of broad array of tumors as a first-line therapy, either alone or in combination with other targeted therapies. The clinical application of doxorubicin, however, is often limited due to its dose-dependent toxicities, such as cumulative cardiotoxicity, myelosuppression, nephrotoxicity, and extravasation.^{1,2} These side effects are closely related to the nonselective distribution of the drug throughout the body following administration.³ Therefore, many efforts have been made to deliver doxorubicin specifically to the tumor by introducing certain targeting moieties that can recognize tumor-specific ligands; this is called active targeting.^{4–8} Clinical findings have demonstrated significant variations among tumor cells within a single tumor mass at both genomic and epigenomic levels.^{9,10} This key issue severely compromises the eligibility of active tumor targeting in the delivery of doxorubicin or any other chemotherapeutic agents. The genomic diversity of the tumor cells within a tumor limits the active targeting approach, to only allowing a fraction of the cell population to be affected; here, only the tumor

subclone expressing the target ligand would be affected.¹¹ The conventional method that is used to investigate the genomic landscape of a tumor in clinical settings is either a single needle biopsy or surgical excision of a very small portion of the tumor tissue. However, this does not take into account the genetically heterogeneous subclones that are spatially separated within the tumor tissue.¹² It is important to note that tumor models induced in preclinical animals are likely to have a genetically homogeneous population of tumor cells. Generally speaking, agents that target tumor-specific ligands show high levels of success in these models. However, they often cannot achieve the same level of therapeutic benefit at the clinical stage, and we believe that intratumor heterogeneity is the chief issue that hinders their success.¹³

For effective and reliable delivery of chemotherapeutic agents (i.e., doxorubicin) to tumors, we previously proposed a strategy of targeting radiation-induced tumor cell apoptosis to deliver such drugs.^{14,15} This strategy aims to target caspase-3, which is

Received: March 16, 2015

Published: August 11, 2015



a cysteine protease that is upregulated in apoptotic cells.¹⁶ By utilizing caspase-3 to activate the prodrug only at the target site, this method does not solely rely on passive methods such as ligand-targeting but can be controlled by exogenous stimuli, i.e., radiation.^{14,15} A further advantage of this method would be the upregulation of caspase-3 by doxorubicin-induced tumor cell death, which would result in amplification of caspase-3 release after their initial expression following the radiation stimuli (Figure 1A).^{17,18}

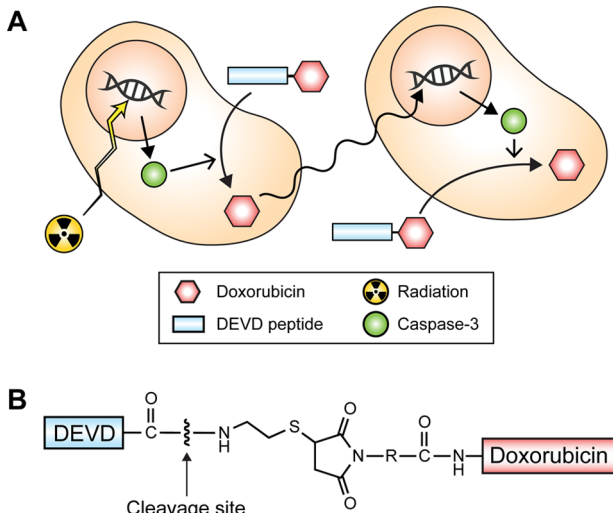


Figure 1. (A) Schematic illustration of the caspase-3-mediated apoptosis targeted doxorubicin prodrug system. (B) Representative structure of the doxorubicin prodrug and the site of cleavage by caspase-3.

Caspase-3 specifically recognizes tetrapeptide (P4–P1) sequences of Asp-Xaa-Xaa-Asp (e.g., DEVD) and hydrolyzes the amide bond following the P1 position Asp residue.^{19–21} Therefore, doxorubicin should be chemically conjugated to the C-terminus of the tetrapeptide, in order to prepare a prodrug that can be activated by caspase-3. However, a direct conjugation of the two molecules is unfavorable considering the presence of a bulky residue in the P1' position of the peptide that results in a significantly decreased substrate-specificity for caspase-3.²² Instead, incorporating a spacer molecule between them is preferred for the prodrug to be specifically activated by caspase-3. In our previous study, doxorubicin was conjugated to the DEVD peptide via *p*-aminobenzylcarbamate (PABC), a self-immolative spacer.¹⁵ Its synthesis inevitably involves subsequent protection and deprotection of the side chain carboxyl groups on the DEVD peptide. However, due to the chemically labile nature of doxorubicin, general methods of protection and deprotection are inappropriate. Alternatively, the carboxyl groups were protected by an allyl ester and deprotected using $Pd(PPh_3)_4$ in a relatively mild condition.¹⁵ However, this resulted in a complicated procedure and a low production yield, which is a great disadvantage when considering the high cost of doxorubicin and the peptide. Moreover, the PABC linker is relatively unstable,²³ which could lead to spontaneous degradation of the compound during circulation and result in off-target activation of the prodrug.

In an attempt to synthesize a more affordable and stable DEVD-conjugated doxorubicin prodrug, we employed a heterobifunctional linker that bears an NHS ester and

maleimide group conjugate and a C-terminus thiolated DEVD peptide (Figure 1B). The caspase-3-mediated cleavage of this prodrug conformation results in the release of a thiol-bearing and linker-conjugated form of doxorubicin rather than free doxorubicin. Thus, several commercially available heterobifunctional linkers differing in length and hydrophobicity were examined. Following trials of adopting various linkers, an appropriate linker was selected based on the *in vitro* biological activities of the expected active forms. According to these results, the final chemical structure of the prodrug was determined and the prodrug thus synthesized using the selected linker. The caspase-3-mediated activation of the prodrug was evaluated *in vitro* by monitoring the prodrug before and after caspase-3 treatment using an analytical HPLC. The cytotoxicity and the cellular uptake of the prodrug in the absence of or in the presence of caspase-3 on MDA-MB-231 breast cancer cells were also determined. Finally, animal studies were carried out in tumor bearing mouse models, which were accompanied by radiation treatment in order to evaluate the therapeutic effect of the newly synthesized doxorubicin prodrug in preclinical models.

RESULTS

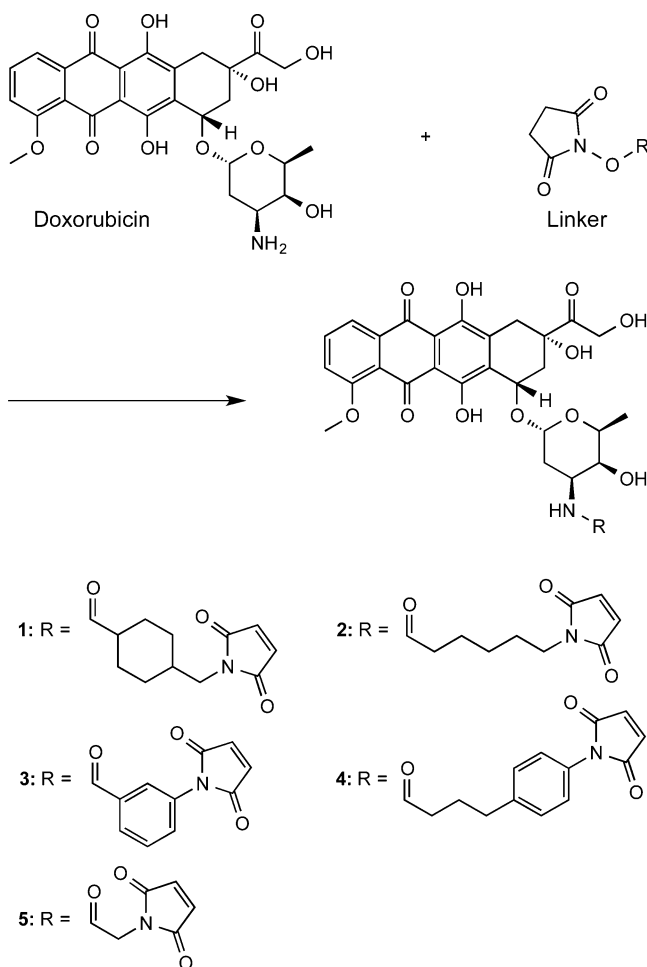
Chemistry. Scheme 1 depicts the synthesis of maleimide derivatives of doxorubicin. Heterobifunctional linkers with NHS ester at one end and maleimide at the other were attached to the primary amine group of the daunosamine sugar moiety of doxorubicin via an amide bond. Doxorubicin hydrochloride was reacted with several different heterobifunctional linkers, which are succinimidyl 4-(*N*-maleimidomethyl)cyclohexane-1-carboxylate (SMCC), *N*-(*ε*-maleimidocaproyloxy)succinimide ester (EMCS), *m*-maleimidobenzoyl-*N*-hydroxysuccinimide ester (MBS), succinimidyl 4-(*p*-maleimidophenyl)butyrate (SMPB), and *N*-(α -maleimidoacetoxymethyl)succinimide ester (AMAS), in the presence of Et_3N to afford maleimide derivatives of doxorubicin 1, 2, 3, 4, and 5, respectively. The products were purified by silica gel flash chromatography using CH_2Cl_2 and CH_3OH (15 v/v%).

To compare the effect of the presence of carboxylic acid in the activated form of our prodrug system, commercially available cysteine and cysteamide hydrochloride were reacted with 1 to yield 6 and 7, respectively, at neutral pH conditions (Scheme 2). To compare the effect of the structure of the heterobifunctional linkers, cysteamide hydrochloride was additionally reacted with 2, 3, 4, and 5 to yield 8, 9, 10, and 11, respectively (Figure 2). The products were purified by reverse phase HPLC using water and CH_3CN with 0.1% TFA as an additive in linear gradient conditions.

Hydrophobicity of the synthesized compounds 7–11 was determined using the *n*-octanol/water shake flask method to identify any correlation between the hydrophobicity of the compounds and their biological activity (Table 1). The results showed that compound 10 had the highest log *P* value and that compound 11 had the least. The order of the hydrophobicity of the analyzed compounds shown by the partition coefficient was also supported by the retention time shown in the reverse phase analytical HPLC (See Supporting Information). The results showed no correlation between the hydrophobicity of the compounds and their biological activities (shown in the following studies).

According to the following studies, we selected compound 3 to react with peptide 12 to obtain the final product 13 (Scheme 3). Compound 3 was reacted with 12 in neutral pH at 4 °C,

Scheme 1. General Synthesis of Maleimide Derivatives of Doxorubicin via Amide Linkage^a

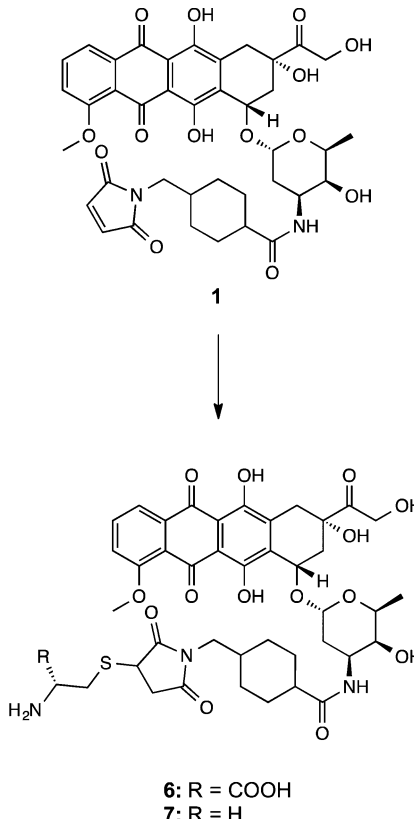


^aReagents and conditions: Et₃N, DMF, 2 h at room temperature in the dark.

and the resulting product was purified by the reverse phase HPLC under the same conditions as those described above.

Biological Activity and Cellular Uptake of 6 and 7. A set of *in vitro* studies was done to evaluate the effect of carboxylic acid in the doxorubicin derivatives. We have prepared two doxorubicin derivatives, compounds **6** and **7**, which share an identical structure except for the fact that **7** lacks one carboxylic group of **6** in the cysteine moiety. We performed the MTT cytotoxicity assay on MDA-MB-231 cells with doxorubicin and compounds **6** and **7** at a concentration range of 0.1–100 μ M to compare their antiproliferative activity (Figure 3A). The results showed that **6**, which has a carboxylic group, did not affect the viability of the MDA-MB-231 cells up to 100 μ M, whereas doxorubicin showed a potent antiproliferative effect. Compound **7**, however, showed a dose-dependent antiproliferative effect, although the potency was significantly lower than that of doxorubicin. We further observed the cellular uptake of doxorubicin and compounds **6** and **7** in MDA-MB-231 cells under confocal microscopy to evaluate the intracellular distribution (Figure 3B; see also Figure S1). Doxorubicin was specifically accumulated in the cell nucleus, showing complete overlap with the DAPI stain. Compound **6**, which showed negligible activity, was mainly distributed in the cytoplasm but not in the nucleus. However, compound **7** was

Scheme 2. General Synthesis of the Expected Compound after Activation of the Doxorubicin Prodrug System by Coupling Cysteine of Cysteamide to the Maleimide Derivative of Doxorubicin^a



^aReagents and conditions: DMF, 4 h at room temperature in the dark.

distributed both in the cytoplasm and nucleus. However, the amount of **7** in the nucleus was significantly less than that of doxorubicin. Through this study, we decided to use cysteamine as a thiol-bearing molecule, rather than cysteine.

Biological Activity and Cellular Uptake of 7–11. We compared the antiproliferative activity and the nuclear accumulation of **7**, **8**, **9**, **10**, and **11**, which differ in their employed heterobifunctional linker, to select the most appropriate linker for the prodrug. The MTT cytotoxicity assay was carried out on MDA-MB-231 cells at a concentration range of 0.1–100 μ M (Figure 4A). The results showed that compound **8**, whose EMCS was employed as a linker, had the most potent antiproliferative activity ($IC_{50} = 4.6 \mu$ M), while the other screened compounds had IC_{50} values over 100 μ M. The observed antiproliferative activity of each compound was closely correlated with the accumulation of the compound in the cell nucleus (Figure 4B; see also Figure S1). In an agreement with the highest antiproliferative activity, compound **8** showed the most specific accumulation in the cell nucleus among the screened compounds (Figure 4C). Other compounds showed almost uniform distribution throughout the nucleus and cytoplasm. Interestingly, compound **11**, which was initially expected to have the most potent activity, as it had the smallest linker employed, showed the least activity and nuclear accumulation. However, although compound **8** had the most potent antiproliferative activity, the activity was lower than that of the intact doxorubicin ($IC_{50} = 0.85 \mu$ M).

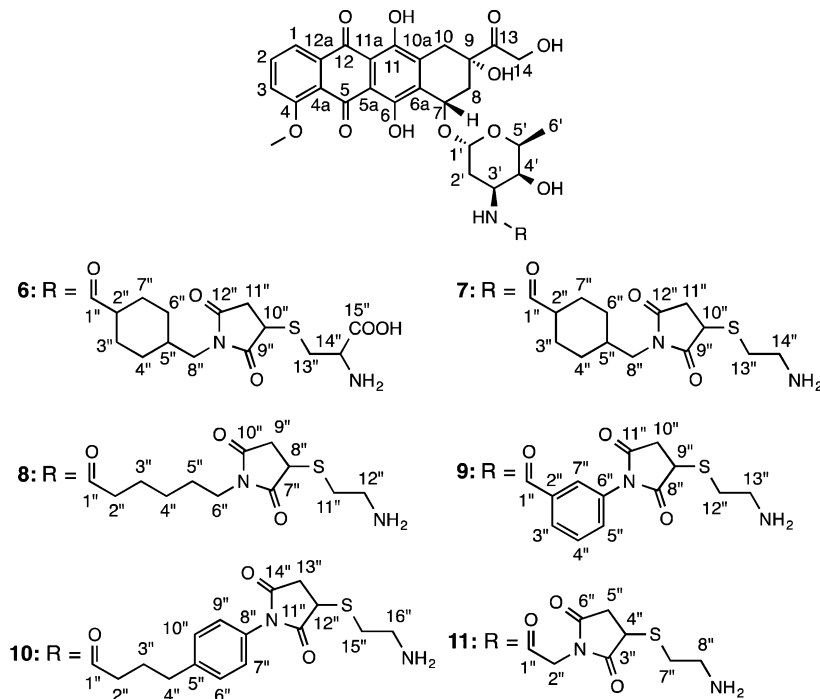


Figure 2. Chemical structures of the active form of the prodrug with different heterobifunctional linkers adopted.

Table 1. Octanol/Water Partition Coefficient of Compounds 7–11^a

compd	7	8	9	10	11
log <i>P</i>	-0.022 ± 0.067	-0.383 ± 0.054	-0.121 ± 0.099	0.313 ± 0.114	-1.041 ± 0.111

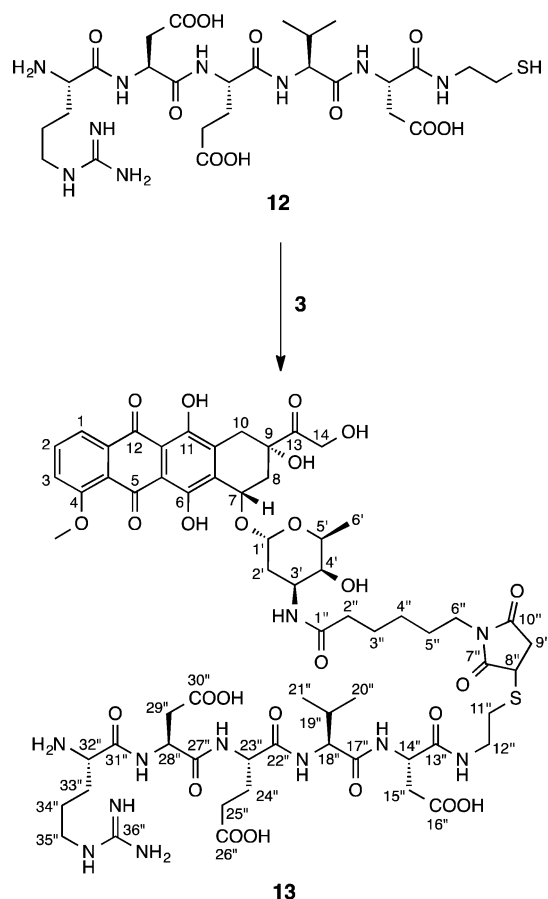
^aData are presented as the mean \pm SD.

In Vitro Caspase-3-Mediated Activation of 13. On the basis of the preceding results, we prepared prodrug 13 by conjugating peptide 12 and doxorubicin via an EMCS linker (**Scheme 3**). The prodrug should be cleaved and activated by caspase-3, which recognizes the DEVD sequence and cleaves the amide bond following aspartic acid, to accomplish its suggested function (**Figure 1B**). Herein, we evaluated the capability of prodrug 13 activation in the presence of caspase-3 *in vitro*. Prodrug 13 was incubated with commercially available purified recombinant human caspase-3 and subjected to HPLC analysis with a fluorescent detector at 470/580 nm, which could detect the intrinsic fluorescence from the doxorubicin moiety (**Figure 5A**). In the HPLC analysis, prodrug 13 showed a single peak at 21.4 min. When prodrug 13 was incubated with caspase-3, however, another peak was detected at 20.6 min. The retention time of this peak was identical to that of compound 8, which was expected to have the same chemical structure with the active substance of the prodrug, manifesting the fact that the caspase-3-mediated cleavage of prodrug 13 released compound 8. In our experimental conditions, more than 98% of the prodrug 13 was converted to compound 8, and only trace amounts of prodrug 13 was found after 30 min of incubation in the presence of caspase-3 (**Figure 5B**). When prodrug 13 was incubated for an hour in the absence of caspase-3, neither conversion to compound 8 nor any degradation was observed, indicating that the conversion of prodrug 13 to compound 8 in the presence of caspase-3 was not responsible for any nonspecific degradation during incubation. These results were further supported by the fact that the incubation of prodrug 13 with caspase-3, which was pretreated with caspase-3 inhibitor (Ac-DEVD-CHO), did not

show any conversion of prodrug 13 to compound 8, manifesting the fact that the conversion of prodrug 13 to compound 8 was caspase-3 specific (**Figure 5A**).

We further performed an MTT cytotoxicity assay to evaluate the antiproliferative activity of prodrug 13 in the presence or absence of caspase-3 (**Figure 5C**). As we hoped, in the absence of caspase-3, the prodrug did not show any noticeable antiproliferative activity up to 10 μ M and showed only minimal activity at 100 μ M in MDA-MB-231 cells. In fact, confocal microscopy showed that when prodrug 13 was incubated with MDA-MB-231 cells, the substance was exclusively found in the cytoplasm but not accumulated in the nucleus (**Figure S2**). However, in the presence of caspase-3, the prodrug showed antiproliferative activity similar to that of compound 8. We further evaluated the intracellular distribution of prodrug 13 with or without caspase-3 treatment *in vitro* on MDA-MD-231 cells by using confocal microscopy (**Figure 5D**; see also **Figure S3**). To observe the behavior of the DEVD moiety as well as the doxorubicin moiety in the cell, we labeled the N-terminus of the peptide moiety of prodrug 13 with Cyanine5.5 fluorescent dye. Our results showed that in the absence of caspase-3, the fluorescent signals from the DEVD moiety and doxorubicin moiety were located mainly in the cytoplasm of the cells and that the two signals (red and green) completely overlapped. This indicated that the two segments of the prodrug were not separated in the absence of caspase-3 and that they did not penetrate inside the cell nucleus. In the presence of caspase-3, however, the fluorescent signals from the doxorubicin moiety were found in the cell nucleus, whereas the signals from the DEVD moiety were only found in the cytoplasm, indicating that the doxorubicin moiety was cleaved

Scheme 3. Synthesis of Prodrug 13 by Conjugating Doxorubicin and a Peptide via an EMCS Linker^a



^aReagents and conditions: DMF, 16 h at 4 °C in the dark.

from the prodrug by caspase-3 and had penetrated into the cell nucleus.

In Vitro Biological Activity of Prodrug 13 with Radiation. To examine the effect of prodrug 13 accompanied by radiation treatment *in vitro*, the MTT cytotoxicity assay was performed on MDA-MB-231 cells (Figure 6A). As previously observed, prodrug 13 had no noticeable antiproliferative effect when treated independently until 48 h of treatment. When MDA-MB-231 cells were exposed to a single dose of a 5 Gy linear X-ray, the number of viable cells decreased below 60% at 48 h of exposure to radiation. The antiproliferative effect of prodrug 13 combined with a single dosing of radiation (linear X-ray, 5 Gy) had no significant difference from that of the radiation-only treated group for 24 h after the treatment. However, at 48 h of treatment, the viable cells decreased by 75% when compared to that of the control group, which also showed 53% decrease when compared to that of the radiation-only treated group, indicating a significant synergistic effect between prodrug 13 and radiation treatment. A certain period of time may have been required for a sufficient concentration of caspase-3 to be upregulated after the initial dosing of radiation on the cells for activation of prodrug 13. This was further supported by the observation of cellular distribution of the prodrug 13 in MDA-MB-231 cells that are exposed to X-rays (Figure 6B). At 6 h postexposure to radiation, no fluorescent signals from the doxorubicin moiety were found in the cell nucleus. However, at 24 h postexposure, the fluorescent signals

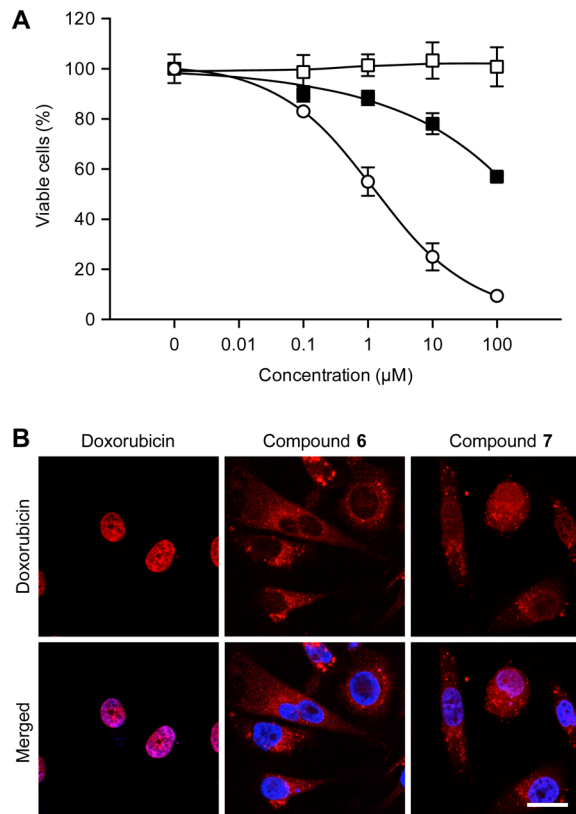


Figure 3. Biological activities of compounds 6 and 7 that differ in the presence of carboxylic acid in their structure. (A) Antiproliferative activity of doxorubicin (○) and compounds 6 (□) and 7 (■) on MDA-MB-231 cells at a concentration range of 0.1–100 μM. (B) Cellular uptake of the compounds in MDA-MB-231 cells. Red and blue fluorescence represent the doxorubicin moiety and the nucleus, respectively. Scale bar, 100 μm.

from doxorubicin were found in the cell nucleus, and the morphology of the cells started to alter, indicating that prodrug 13 was cleaved and that the released doxorubicin moiety was accumulated in the nucleus as the cells underwent apoptosis after exposure to radiation. Indeed, when the cells were exposed to radiation, caspase-3 was upregulated in a time-dependent manner (Figure 6C). This clearly showed that caspase-3 upregulated during apoptosis that is induced by radiation activated prodrug 13 and allowed the released doxorubicin moiety (equivalent to compound 8) to be accumulated in the cell nucleus.

Caspase-3 Cellular Activation. The upregulation of caspase-3 in MDA-MB-231 cells when treated with prodrug 13, activated prodrug 13, or compound 8 was evaluated by Western blot (Figure 6D; full-length blots are shown in Figure S4). The results showed that activated prodrug 13, which is prodrug 13 preincubated with commercially available purified caspase-3, and compound 8, which is a synthesized equivalent of activated prodrug 13, increased the amount of cleaved caspase-3 in a dose-dependent manner (also known as activated caspase-3) and decreased the amount of procaspase-3 in MDA-MB-231 cells, indicating that cell death by activated prodrug 13 occurred via caspase-3-mediated apoptosis. However, the prodrug 13 itself showed no increase of cleaved caspase-3 up to a concentration of 100 μM, supporting the results of the MTT cytotoxicity assay, which showed only negligible antiproliferative effects of prodrug 13. These results manifested

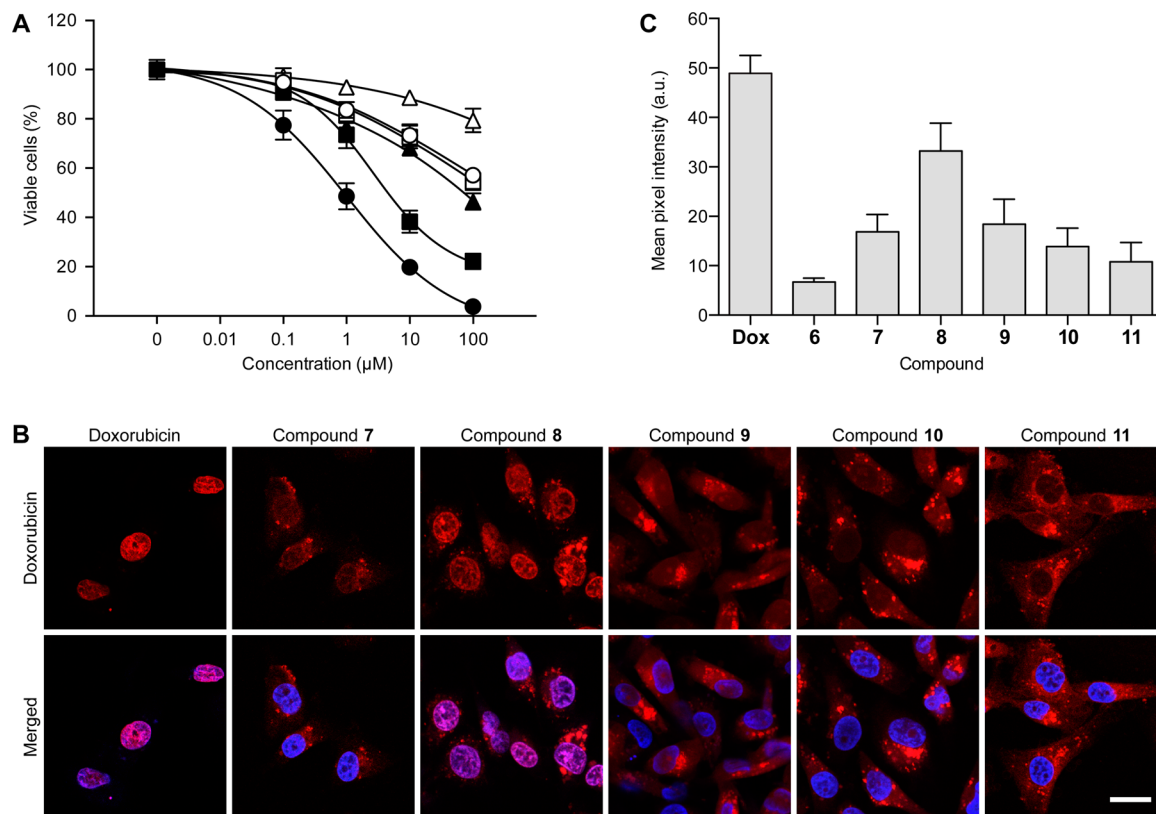


Figure 4. Biological activities of compounds 7–11 that differ in the employed heterobifunctional linker within their molecules. (A) Antiproliferative activity of doxorubicin (●) and compounds 7 (○), 8 (■), 9 (□), 10 (■), and 11 (△) in MDA-MB-231 cells at the concentration range of 0.1–100 μM . (B) Cellular uptake and intracellular distribution of the compounds in MDA-MB-231 cells. Red and blue fluorescence represent the treated compounds and cell nucleus, respectively. Scale bar, 100 μm . (C) Quantitatively measured fluorescent intensity of compounds 7–11 in the cell nuclei.

our initial hypothesis that the prodrug could be continuously activated in the site where apoptosis was induced initially since activated prodrug 13 could again activate caspase-3, which could repeatedly lead the cleavage of another molecule of prodrug 13.

Animal Study. Tumor suppression effect of prodrug 13 was evaluated *in vivo* with SCC7 tumor-bearing Balb-c/nu mice (Figure 7). When tumors were grown to a size of 100 mm^3 , they were exposed to 10 Gy linear X-rays on the first day of drug administration. Prodrug 13 was administered daily intravenously for 7 days. The tumor growth in the group that received only prodrug 13 without exposure to radiation had no significant difference with the control group that received saline. The mean tumor volume at the final measuring point was decreased only by 15% when compared to that of the control. The tumors that were exposed to a single dose of 10 Gy radiation without administration of the prodrug decreased by 53% in their volume when compared to that of the control. However, when prodrug 13 was treated after a single dose of 10 Gy radiation, tumor volume was decreased by 79% compared to that of the control, which was decreased 54% compared to that of the radiation-only group. The results showed a significant synergistic effect of prodrug 13 when accompanied by an initial radiation exposure in suppressing tumor growth *in vivo*. All of the tested groups showed no decrease in their body weight, indicating that there was no significant toxicity in any experimental groups during the course of the study.

DISCUSSION

The present study demonstrates optimal structure determination and also preparation of a DEVD peptide conjugated doxorubicin prodrug that could be easily synthesized by incorporating a heterobifunctional linker. There are several ways to conjugate the linker to doxorubicin, including the formation of an amide bond on the 3'-amino position or a hydrazone bond on the 13-keto position of doxorubicin.^{24,25} Among the many methods, this particular method was selected to produce a stable conjugate, which could prevent nonspecific or off-target cleavage of the final compound. We also modified the peptide slightly: the C-terminus was thiolated by adding Cys or cysteamide at the P1' position. Finally, a heterobifunctional linker that has the NHS ester and maleimide group was used to connect doxorubicin and the peptide. Such reactions could be carried out in mild conditions with minimal reaction steps and do not involve any protection and deprotection of the carboxyl groups of the peptide; overall, this leads to a high production yield (73.8%) of the final product. However, the major disadvantage of using the stable heterobifunctional linker is that its cleavage by caspase-3 releases the entire residue after the P1 Asp of the conjugate rather than free doxorubicin (see Figure 1B). Since the 3'-amino group of doxorubicin plays a significant role in the stabilization of the doxorubicin–DNA complex, the decreased biological activity of the released active compound, when compared to that of free doxorubicin, is unavoidable.^{26,27} Therefore, we prepared several active compound candidates of the prodrug (compound 6–11) that differ in their thiolated residue or linker residue and examined

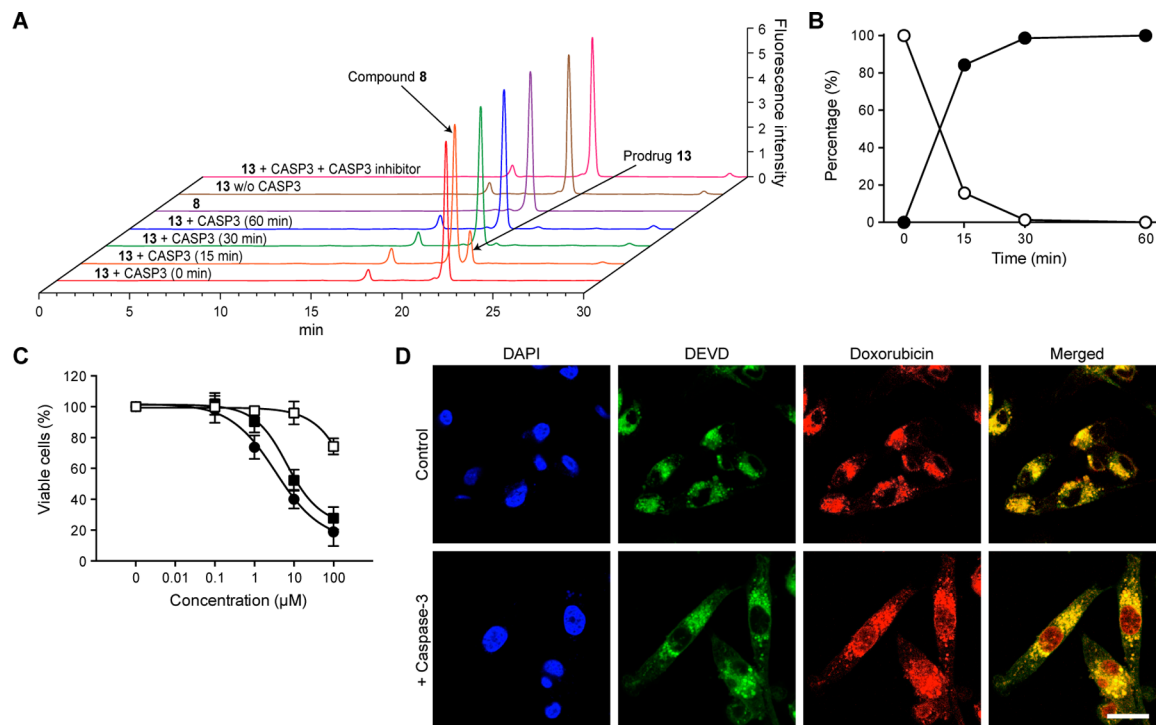


Figure 5. (A) Chromatograms of prodrug **13** incubated with recombinant human caspase-3. Chromatograms of compound **8**, prodrug **13** incubated without caspase-3 for 60 min and prodrug **13** incubated with caspase-3 that is pretreated with caspase-3 inhibitor (Ac-DEVD-CHO) are also shown. (B) Percent ratio of prodrug **13** (○) and compound **8** (●) during incubation in the presence of caspase-3 by time. (C) Antiproliferative activity of compound **8** (●) and prodrug **13** in the presence (■) or absence (□) of caspase-3 in MDA-MB-231 cells at a concentration range of 0.1–100 μM . (D) Intracellular distribution of prodrug **13** in the presence or absence of caspase-3 in MDA-MB-231 cells. Green, red, and blue fluorescence represent DEVD peptide moiety, doxorubicin moiety, and cell nucleus, respectively. Scale bar, 100 μm .

their biological activities. Accordingly, the structure of the prodrug was determined that would incur the least amount of loss in its biological activity after activation. Comparison of the biological activity between compounds **6** and **7** showed that the presence of $-\text{COOH}$ in the molecule was unfavorable due to its nucleus accumulation and the compounds' antiproliferative activity. DNA is negatively charged by the phosphate backbone, thus the negatively charged carboxyl group of the compound could hamper their interaction with DNA by electrostatic repulsion. Moreover, when exploring the influence of the adopted linker, we found that the EMCS linker least affected the biological activity of the doxorubicin when conjugated. No correlation between hydrophobicity and the biological activities of the active compounds were found. Rather, the flexibility of the linkers was deemed to significantly contribute to their activity. The 3'-amino group, which is critical for the biological activity of doxorubicin,²⁷ is acylated by the conjugated linker in the synthesized active compounds, resulting in the loss of its function. Instead, the compounds possessing an alternative primary amino group at the end of the linker may have contributed to the stabilization of the DNA–doxorubicin derivative complex. Compounds **7**, **9**, and **10** have a cyclohexane or a benzene ring between the pyrrolidine and the daunosamine sugars of the doxorubicin moiety that restricts the movement of the terminal amine group via steric hindrance. In contrast, compound **8** has an alkane that provides a higher extent of flexibility that allows the amino group to move more freely. This could result in an increased possibility of the amine group interacting with DNA, thereby showing the highest biological activity among the synthesized compounds. Interestingly, compound **11** also retains an alkane linker, but it showed

a significantly lower activity than **8**. This could be explained by the difference in the length of the linkers, which determines the distance between the pyrrolidine ring and the daunosamine sugar of doxorubicin. Unlike compound **8**, the pyrrolidine ring and the sugar moiety of doxorubicin of compound **11** are very close to each other, which could limit the flexibility of the linker due to steric hindrance.

On the basis of these results, we chose compound **8** as the active compound of the prodrug. Therefore, prodrug **13** was prepared by conjugating the DEVD-cysteamide **12** and doxorubicin via an EMCS linker. Our *in vitro* studies showed that caspase-3 cleaved prodrug **13** and released compound **8**, which was inhibited when the caspase-3 inhibitor (Ac-DEVD-CHO) was pretreated with caspase-3. This result exhibited that caspase-3 specifically recognized the DEVD motif and hydrolyzed the amide bond following P1' Asp, subsequently releasing the active substrate as expected. As a result, prodrug **13** transformed from an inactive form to the active compound that showed equivalent antiproliferative activity with synthetic compound **8** on MDA-MB-231 cells in the presence of caspase-3. Observation of the intracellular distribution of prodrug **13** showed that caspase-3 stimulated the accumulation of doxorubicin inside the cell nucleus, whereas the intact prodrug was almost exclusively found in the cytoplasm. Also, the DEVD moiety remained in the cytoplasm when prodrug **13** was cleaved. This suggested that the DEVD moiety limited prodrug **13** from accumulating in the nucleus, hence rendering the prodrug inactive. The DEVD motif has three $-\text{COOH}$ groups in its amino acid side chains. As the $-\text{COOH}$ is generally ionized in physiological pH, the side chain $-\text{COOHs}$ would restrict the penetration of prodrug **13** through the lipid

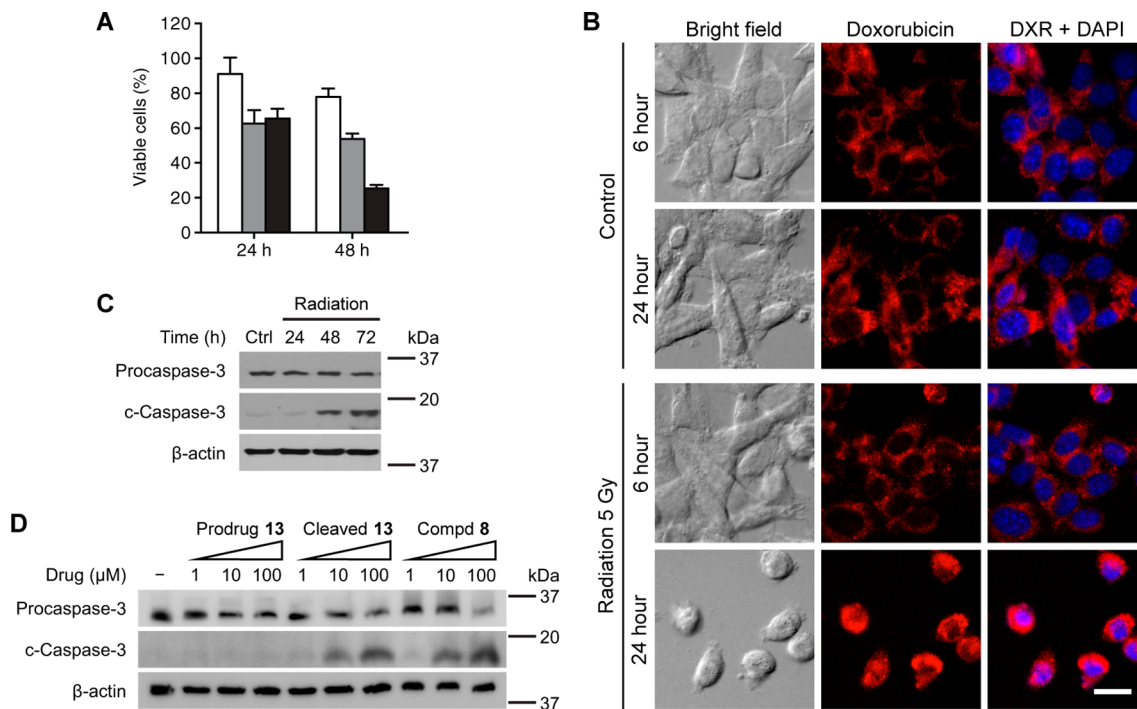


Figure 6. Biological activity of prodrug 13 when accompanied by radiation exposure on MDA-MB-231 cells. The final concentration of prodrug 13 during treatment was 5 μ M and the dose of given radiation (X-ray) was 5 Gy. (A) Antiproliferative activity prodrug 13 with (black) or without (white) radiation, and only radiation (gray) without drug treatment on MDA-MB-231 cells. The cells were incubated for 24 and 48 h post-treatment. (B) Intracellular distribution of prodrug 13 with or without radiation treatment on MDA-MB-231 cells. Red and blue fluorescence represent the doxorubicin moiety and the nucleus, respectively. Scale bar, 100 μ m. Western blot of procaspase-3 (35 kDa) and cleaved caspase-3 (c-Caspase-3; 17 kDa) of MDA-MB-231 cells exposed to radiation (C), and the cells treated with prodrug 13, activated prodrug 13 (prodrug 13 preincubated with commercially available caspase-3), or compound 8 (D).

bilayer membrane of the nuclear envelope. The augmentation of the total molecular size by the added DEVD motif may also contribute to the lowered penetration of prodrug 13 when compared to that of compound 8. Furthermore, the net negative charge given by the DEVD moiety within prodrug 13 could potentially discourage the interaction with the negatively charged DNA by electrostatic repulsion, even after its penetration inside the nucleus. The caspase-3-mediated cleavage of the DEVD moiety from the prodrug removes the negative charge and also leads to decrease in molecular size, thereby allowing the doxorubicin moiety to easily penetrate into the nucleus and bind DNA.

Our subsequent studies demonstrated that prodrug 13 showed significant synergistic effect when accompanied by radiation *in vitro* and *in vivo*. It has been recognized that irradiated tumor cells undergo apoptosis and release caspases, including caspase-3, which was also shown in our study.^{15,28} Our studies showed that prodrug 13 did not have any noticeable biological activity without any exogenous stimuli. Only when purified caspase-3 or radiation was given to cells, the tumor, or the animal did prodrug 13 initiate its therapeutic activity.

Although *in vitro* studies of compound 8, the active substance of prodrug 13, showed lower antiproliferative activity than doxorubicin, prodrug 13 showed satisfactory anticancer effect *in vivo* when accompanied by radiation treatment. Since doxorubicin has nonselective tissue distribution characteristic with a high volume of distribution, the amount of the agent reaching the tumor tissue specifically would be relatively smaller than that in normal organs, resulting in high toxicity.³ However, our *in vitro* studies showed that prodrug 13 did not

readily accumulate in cells and their nucleus, except when the cells were exposed to radiation. Therefore, during the circulation of prodrug 13 in the body, it could specifically accumulate in the irradiated tissue (i.e., tumor) rather than the normal tissue. Moreover, the prodrug is less likely to accumulate in the cells before it activates. Thus, it would bypass the normal tissue and potentially higher amounts of the drug could reach the tumor, where it could be activated and accumulated. By the same token, the prodrug would have a lower toxicity profile than doxorubicin. Indeed, when the prodrug was administered to mice in molar equivalent doses of 5 mg/kg of doxorubicin, all the tested mice survived without any noticeable body weight change until the last day of observation (14 days), while doxorubicin-treated mice were all dead within 6 days (Figure S5). Our previous study has also demonstrated that when doxorubicin is coupled with the DEVD peptide, lower toxicity on the normal organs were observed compared to that with doxorubicin alone.¹⁵

Throughout the study, we showed that prodrug 13 could significantly potentiate radiation therapy with less toxicity, by the fact that the drug would only activate at the irradiated site, where part of the tumor cells undergoes apoptosis. The activation of the prodrug relies on caspase-3 upregulation during apoptosis, which is a common pathway in mammalian cells, rather than the genomic properties of tumor cells. Hence, it may overcome the limitation of targeted therapy or active targeting that is caused by the genomic heterogeneity of tumor cell population. The optimization of the prodrug allowed it to be easily synthesized in high production yield with reasonable biological activity, thereby making it more commercially affordable. The prodrug suggested in this study would be a

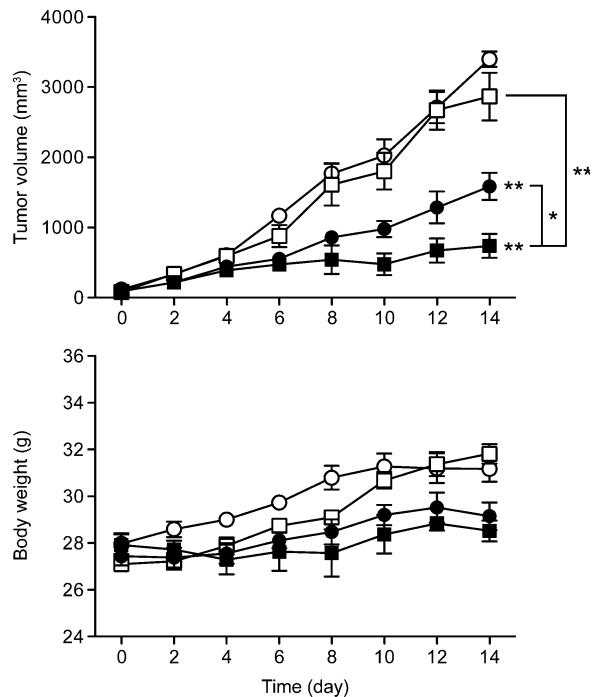


Figure 7. Animal studies on SCC7 tumor-bearing mice. (A) Tumor growth of control (○), prodrug 13 (□; 5 mg/kg; daily i.v. administration for 7 days), radiation only (●; 10 Gy single exposure of linear X-ray at the starting point of the experiment), and combination of prodrug 13 and radiation (■; identical dose and dosing schedule as described above). (B) Body weight measurement of each group. Data are expressed as the means \pm SEM. * P < 0.05, ** P < 0.005 versus the control or as specified.

promising anticancer agent for the treatment of local tumors by effectively delivering doxorubicin when used in combination with radiation therapy.

In the future studies, the therapeutic effect of the prodrug will be tested in various types of cancer cells, including radio-sensitive and radio-resistant cell lines. In-depth preclinical toxicity studies are also planned to evaluate the eligibility of the prodrug for clinical trials. In addition, considering the fact that current application of the prodrug is limited to local tumors that could be treated with radiation therapy, we are seeking a distinct treatment method to apply the prodrug in distal metastatic tumors.

EXPERIMENTAL SECTION

General Synthesis. All solvents and Et₃N were purchased from Sigma-Aldrich (St. Louis, MO). Succinimidyl 4-(N-maleimidomethyl)-cyclohexane-1-carboxylate (SMCC), N-(ϵ -maleimidocaproyloxy)succinimide ester (EMCS), m-maleimidobenzoyl-N-hydroxysuccinimide ester (MBS), succinimidyl 4-(p-maleimidophenyl)butyrate (SMPB), and N-(α -maleimidooacetoxy)succinimide ester (AMAS) were obtained from Pierce (Rockford, IL). Doxorubicin hydrochloride was kindly provided by Dong-A ST (Seoul, South Korea). To the solution of doxorubicin hydrochloride (20 mg, 34.48 μ mol, 1.2 equiv) in anhydrous DMF (1 mL), Et₃N (10 μ L, 71.84 μ mol, 2.5 equiv) was added and stirred for 30 min at room temperature. SMCC, EMCS, MBS, SMPB, or AMAS (28.74 μ mol, 1 equiv) was added and stirred further for 2 h at room temperature in nitrogen atmosphere in the dark to obtain 1–5, respectively. The reaction was monitored using normal phase TLC ($\text{CH}_2\text{Cl}_2/\text{CH}_3\text{OH}/\text{CH}_3\text{COOH}$, 6:3:1, v/v/v). After the reaction was completed, the solution was diluted 10 times in CH_2Cl_2 and filtered to remove the precipitated doxorubicin. The solution was concentrated and transferred into 10 volumes of diethyl ether to

precipitate the product. The precipitate was collected by filtration and dried to obtain the maleimide derivatives of doxorubicin 1–5 as red solid.

The prepared maleimide derivatives of doxorubicin were dissolved in anhydrous DMF (1 mL) and reacted with cysteamine hydrochloride (16.3 mg, 143.68 μ mol, 5 eq; Sigma-Aldrich) to obtain 7–11. Compound 1 was also reacted with cysteine (17.4 mg, 143.68 μ mol; Sigma-Aldrich) to obtain 6. The solutions were reacted for 4 h at room temperature in the dark. The reaction was monitored using normal phase TLC ($\text{CH}_2\text{Cl}_2/\text{CH}_3\text{OH}/\text{CH}_3\text{COOH}$, 6:3:1, v/v/v). The product was purified using a semipreparative HPLC system (Shimadzu, Kyoto, Japan) with an ODS-A 5 μ m semipreparative column (150 mm \times 20 mm; YMC, Dinslaken, Germany). A gradient system (Water and CH_3CN with 0.05% TFA as an additive) was used at a flow rate of 8 mL/min, and the chromatogram was monitored using a UV detector at 280 nm. The collected fractions were concentrated in reduced pressure and lyophilized to obtain final products as a red powder. The purity of the final products was confirmed by analytical HPLC (Agilent 1300 series, Agilent Technologies, Santa Clara, CA) using an ODS-A 5 μ m analytical column (150 mm \times 3 mm; YMC, Dinslaken, Germany). A gradient system (Water and CH_3CN with 0.1% TFA as an additive, CH_3CN 5–95%/5–30 min) was applied at a flow rate of 0.8 mL/min and monitored under UV (214 nm) and a fluorescent detector (470/580 nm). The purity of the analyzed compounds was determined to be \geq 95%.

Compound 6. Red solid (23.8 mg, 93.7% yield). ¹H NMR (500 MHz, DMSO-*d*₆, δ ppm): 13.94 (s, 1H, 6-OH), 13.18 (s, 1H, 11-OH), 7.84 (dd, J = 7.6, 7.6 Hz, 1H, H2), 7.81 (d, J = 7.6 Hz, 1H, H3), 7.57 (d, J = 7.6 Hz, 1H, H1), 7.38 (d, 1H, 3'-NH), 5.20 (br s, 1H, H1'), 4.87 (br s, 1H, H7), 4.57 (s, 2H, H14), 4.23 (m, 1H, H5'), 4.16 (m, 1H, H5'), 4.08 (m, 1H, H10''), 3.95 (s, 3H, OCH₃), 3.91 (m, 1H, H3'), 3.36 (m, 1H, H4'), 3.20 (m, 2H, H13''), 3.18 (m, 1H, H11''), 3.18 (m, 2H, H8''), 2.95 (d, J = 18.0 Hz, 1H, H10), 2.84 (d, J = 18.0 Hz, 1H, H10), 2.54 (dd, J = 17.0, 4.0 Hz, 1H, H11'), 2.18 (d, J = 14.5 Hz, 1H, H8), 2.05 (d, J = 14.5 Hz, 1H, H8), 2.05 (m, 1H, H2''), 1.83 (dd, 1H, H2''), 1.59 (m, 4H, H3'', H4'', H6'', H7''), 1.46 (m, 1H, H5''), 1.38 (d, J = 13.0 Hz, 1H, H2''), 1.18 (m, 2H, H3'', H7''), 1.12 (d, J = 6.5 Hz, 3H, H6''), 0.87 (m, 2H, H4'', H6''). ¹³C NMR (125 MHz, DMSO-*d*₆, δ ppm): 213.84 (C13), 186.35 (C5), 186.25 (C12), 177.20 (C12''), 175.06 (C9''), 174.30 (C1''), 169.37 (C15''), 160.71 (C4), 156.07 (C11), 154.49 (C6), 136.13 (C2), 135.42 (C12a), 134.51 (C6a), 133.98 (C10a), 119.85 (C4a), 119.63 (C1), 118.90 (C3), 110.65 (C5a), 110.51 (C11a), 100.50 (C1'), 74.94 (C9), 69.91 (C7), 68.15 (C4'), 66.76 (C5'), 63.71 (C14), 56.52 (OCH₃), 52.04 (C14''), 44.72 (C3'), 44.20 (C8''), 43.42 (C2''), 38.77 (C10''), 36.49 (C8), 35.47 (C5''), 35.35 (C11''), 32.01 (C10), 31.53 (C13''), 29.73 (C2''), 29.28 (C4'', C6''), 28.60 (C3'', C7''), 17.01 (C6''). HRMS (ESI-TOF): calcd for C₄₂H₄₉N₃O₁₆S, 883.2834; found 883.2829 (Δ = 0.47 ppm).

Compound 7. Red solid (21.8 mg, 90.1% yield). ¹H NMR (600 MHz, DMSO-*d*₆, δ ppm): 13.95 (s, 1H, 6-OH), 13.19 (s, 1H, 11-OH), 7.85 (dd, J = 7.6, 7.6 Hz, 1H, H2), 7.82 (d, J = 7.6 Hz, 1H, H2), 7.58 (d, J = 7.6 Hz, 1H, H1), 7.36 (d, 1H, 3'-NH), 5.19 (br s, 1H, H1'), 4.88 (br s, 1H, H7), 4.60 (s, 2H, H14), 4.14 (q, J = 6.5 Hz, 1H, H5'), 4.05 (dd, J = 4.0, 9.0 Hz, 1H, H10''), 3.95 (s, 3H, OCH₃), 3.91 (m, 1H, H3'), 3.36 (m, 1H, H4'), 3.19 (m, 1H, H11''), 3.18 (m, 2H, H8''), 3.06 (m, 2H, H14''), 3.02 (m, 2H, H13''), 2.95 (d, J = 18 Hz, 1H, H10), 2.87 (d, J = 18 Hz, 1H, H10), 2.85 (m, 1H, H13''), 2.51 (dd, J = 17.0, 4.0 Hz, 1H, H11'), 2.19 (d, J = 14.5 Hz, 1H, H8), 2.08 (m, 1H, H8), 2.05 (m, 1H, H2''), 1.82 (ddd, J = 13.0, 13.0, 4.5 Hz, 1H, H2''), 1.63 (m, 4H, H3'', H4'', H6'', H7''), 1.49 (m, 1H, H5''), 1.39 (dd, J = 13.0, 4.5 Hz, 1H, H2''), 1.17 (m, 2H, H3'', H7''), 1.12 (d, J = 6.5 Hz, 3H, H6''), 0.85 (m, 2H, H4'', H6''). ¹³C NMR (150 MHz, DMSO-*d*₆, δ ppm): 213.76 (C13), 186.37 (C5), 186.27 (C12), 177.11 (C12''), 175.05 (C9''), 174.26 (C1''), 160.71 (C4), 156.05 (C11), 154.46 (C6), 136.12 (C2), 135.43 (C12a), 134.53 (C6a), 133.97 (C10a), 119.87 (C4a), 119.64 (C1), 118.91 (C3), 110.67 (C5a), 110.52 (C11a), 100.46 (C1'), 74.93 (C9), 69.90 (C7), 68.13 (C4'), 66.75 (C5''), 63.67 (C14), 56.52 (OCH₃), 44.70 (C3''), 44.09 (C8''), 43.40

(C2''), 38.95 (C10''), 38.27 (C14''), 36.51 (C8), 35.42 (C5''), 35.35 (C11''), 32.01 (C10), 29.70 (C2''), 29.29 (C4'', C6''), 28.58 (C3'', C7''), 28.38 (C13''), 16.99 (C6''). HRMS (ESI-TOF): calcd for $C_{41}H_{49}N_3O_{14}S$, 839.2935; found 839.2934 ($\Delta = 0.13$ ppm).

Compound 8. Red solid (21.7 mg, 92.6% yield). 1H NMR (600 MHz, CD_3OD , δ ppm): 7.70 (br s, 2H, H1, H2), 7.41 (br s, 1H, H3), 5.38 (br s, 1H, H1'), 5.00 (br s, 1H, H7), 4.75 (d, $J = 19.5$ Hz, 1H, H14), 4.72 (d, $J = 19.5$ Hz, 1H, H14), 4.24 (q, $J = 6.5$ Hz, 1H, H5'), 4.12 (d, $J = 12.5$ Hz, 1H, H3'), 3.95 (s, 3H, OCH₃), 3.82 (dd, $J = 7.5$, 4.5 Hz, 1H, H8''), 3.60 (s, 1H, H4'), 3.38 (m, 2H, H6''), 3.21 (m, 1H, H12''), 3.17 (m, 1H, H12''), 3.11 (dd, $J = 7.5$, 12.5 Hz, 1H, H9''), 3.06 (m, 1H, H11''), 2.97 (d, $J = 18.0$ Hz, 1H, H10), 2.92 (m, 1H, H11''), 2.79 (d, $J = 18.0$ Hz, 1H, H10), 2.36 (dd, $J = 4.5$, 12.5 Hz, 1H, H9''), 2.33 (d, $J = 14.0$ Hz, 1H, H8), 2.16 (t, $J = 7.5$ Hz, 2H, H2''), 2.12 (d, $J = 14.0$ Hz, 1H, H8), 1.97 (dd, $J = 12.5$, 12.5 Hz, 1H, H2''), 1.73 (d, $J = 12.5$ Hz, 1H, H2''), 1.55 (tt, $J = 7.5$, 7.5 Hz, 2H, H3''), 1.49 (tt, $J = 7.5$, 7.5 Hz, 2H, H5''), 1.27 (d, $J = 6.5$ Hz, 3H, H6''), 1.22 (tt, $J = 7.5$, 7.5 Hz, 2H, H4''). ^{13}C NMR (150 MHz, CD_3OD , δ ppm): 214.59 (C13), 187.80 (C5), 187.50 (C12), 179.13 (C7''), 176.42 (C10''), 175.37 (C1''), 162.32 (C4), 157.20 (C6), 156.02 (C11), 137.15 (C2), 136.14 (C12a), 135.63 (C6a), 135.04 (C10a), 121.31 (C4a), 120.46 (C1), 120.22 (C3), 112.37 (C5a), 112.09 (C11a), 102.28 (C1''), 77.35 (C9), 71.26 (C7), 69.98 (C4''), 66.67 (C5''), 65.73 (C14), 57.10 (OCH₃), 47.03 (C3''), 40.14 (C8''), 39.97 (C12''), 39.69 (C6''), 37.22 (C8), 36.68 (C9''), 36.37 (C2''), 33.98 (C10), 30.54 (C11''), 28.16 (C5''), 27.15 (C4''), 26.37 (C3''), 17.30 (C6''). HRMS (ESI-TOF): calcd for $C_{39}H_{47}N_3O_{14}S$, 813.2779; found 813.2769 ($\Delta = 1.19$ ppm).

Compound 9. Red solid (21.6 mg, 91.8% yield). 1H NMR (500 MHz, CD_3OD , δ ppm): 7.85 (d, $J = 7.8$ Hz, 1H, H3''), 7.74 (m, 1H, H1, H7''), 7.70 (t, $J = 7.8$ Hz, 1H, H2), 7.53 (dd, $J = 7.8$, 7.8 Hz, 1H, H4''), 7.42 (m, 2H, H3, H5''), 5.42 (br s, 1H, H1'), 5.04 (br s, 1H, H7), 4.77 (d, $J = 20.0$ Hz, 1H, H14), 4.71 (d, $J = 20.0$ Hz, 1H, H14), 4.36 (m, 1H, H3''), 4.32 (q, $J = 6.5$ Hz, 1H, H5''), 3.92 (s, 3H, OCH₃), 3.72 (s, 1H, H4''), 3.35 (dd, $J = 3.0$, 18.0 Hz, 1H, H10''), 3.25 (m, 2H, H9'', H13''), 3.20 (m, 2H, H12''), 3.03 (m, 1H, H12''), 3.00 (d, $J = 18.5$ Hz, 1H, H10), 2.85 (d, $J = 18.5$ Hz, 1H, H10), 2.64 (dd, $J = 11.5$, 18.0 Hz, 1H, H10''), 2.36 (d, $J = 15.0$ Hz, 1H, H8), 2.12 (m, 2H, H8, H2''), 1.83 (d, $J = 12.0$ Hz, 1H, H2''), 1.28 (d, $J = 6.5$ Hz, 3H, H2''). ^{13}C NMR (125 MHz, CD_3OD , δ ppm): 214.67 (C13), 187.92 (C5), 187.59 (C12), 178.16 (C11''), 175.36 (C8''), 168.44 (C1''), 162.34 (C4), 157.29 (C6), 156.11 (C11), 137.13 (C2), 136.84 (C6''), 136.22 (C12a), 135.69 (C6a), 135.12 (C10a), 133.72 (C2''), 131.00 (C5''), 130.26 (C4''), 128.55 (C3''), 127.23 (C7''), 121.38 (C4a), 120.47 (C1), 120.18 (C3), 112.38 (C5a), 112.12 (C11a), 102.20 (C1''), 77.36 (C9), 71.23 (C7), 69.89 (C4''), 68.63 (C5''), 65.73 (C14), 57.06 (OCH₃), 48.09 (C3''), 39.95 (C13''), 37.32 (C8), 36.67 (C10''), 34.00 (C10), 30.73 (C12''), 30.38 (C2''), 17.31 (C6''). HRMS (ESI-TOF): calcd for $C_{40}H_{41}N_3O_{14}S$, 819.2309; found 819.2304 ($\Delta = 0.63$ ppm).

Compound 10. Red solid (23.8 mg, 95.9% yield). 1H NMR (500 MHz, CD_3OD , δ ppm): 7.55 (dd, $J = 7.7$, 7.7 Hz, 1H, H2), 7.52 (d, $J = 7.7$ Hz, 1H, H1), 7.25 (d, $J = 7.7$ Hz, 1H, H3), 7.19 (d, $J = 8.2$ Hz, 2H, H6'', H10''), 7.07 (d, $J = 8.2$ Hz, 2H, H7'', H9''), 5.34 (s, 1H, H1'), 4.91 (s, 1H, H7), 4.75 (d, $J = 20.0$ Hz, 1H, H14), 4.71 (d, $J = 20.0$ Hz, 1H, H14), 4.22 (q, $J = 6.5$ Hz, 1H, H5''), 4.13 (d, $J = 12.0$ Hz, 1H, H3''), 4.05 (m, 1H, H12''), 3.83 (s, 3H, OCH₃), 3.62 (s, 1H, H4''), 3.34 (m, 1H, H13''), 3.26 (m, 2H, H16''), 3.21 (m, 1H, H15''), 3.02 (m, 1H, H15''), 2.90 (d, $J = 18.5$ Hz, 1H, H10), 2.68 (d, $J = 18.5$ Hz, 1H, H10), 2.61 (m, 1H, H13''), 2.58 (m, 1H, H4''), 2.29 (d, $J = 15.0$ Hz, 1H, H8), 2.19 (t, $J = 7.5$ Hz, 2H, H2''), 2.04 (d, $J = 15.0$ Hz, 1H, H8), 1.98 (dd, $J = 12.5$, 12.5 Hz, 1H, H2''), 1.84 (tt, $J = 7.5$, 7.5 Hz, 2H, H3''), 1.76 (d, $J = 12.5$ Hz, 1H, H2''), 1.26 (d, $J = 6.5$ Hz, 3H, H6''). ^{13}C NMR (125 MHz, CD_3OD , δ ppm): 214.69 (C13), 187.34 (C5), 187.10 (C12), 178.35 (C14''), 175.62 (C11''), 175.12 (C1''), 162.07 (C4), 157.04 (C6), 155.81 (C11), 143.91 (C8''), 136.99 (C2), 135.80 (C12a), 135.41 (C6a), 134.86 (C10a), 131.17 (C5''), 130.10 (C6''), 127.70 (C7''), 127.0 (C9''), 120.97 (C4a), 120.33 (C1), 120.01 (C3), 112.11 (C5a), 111.88 (C11a), 102.21 (C1''), 77.36 (C9), 71.06 (C7), 69.89 (C4''), 68.63 (C5''), 65.77 (C14), 57.02 (OCH₃), 47.10 (C3''), 41.02 (C12''), 39.94 (C16''), 37.11 (C8), 36.73 (C13''), 36.33 (C2''), 35.75 (C4''), 33.98 (C10), 30.71 (C15''), 30.44 (C2''), 28.56

(C3''), 17.33 (C6''). HRMS (ESI-TOF): calcd for $C_{43}H_{47}N_3O_{14}S$, 861.2779; found 861.2766 ($\Delta = 1.43$ ppm).

Compound 11. Red solid (20.8 mg, 92.2% yield). 1H NMR (600 MHz, CD_3OD , δ ppm): 7.72 (m, 2H, H1, 2), 7.45 (m, 1H, H3), 5.38 (s, 1H, H1'), 5.02 (s, 1H, H7), 4.74 (d, $J = 20.0$ Hz, 1H, H14), 4.70 (d, $J = 20.0$ Hz, 1H, H14), 4.23 (q, 1H, H5''), 4.18 (s, $J = 6.5$ Hz, 2H, H2''), 4.15 (m, 1H, H3''), 3.98 (m, 1H, H4''), 3.97 (s, 3H, OCH₃), 3.60 (s, 1H, H4''), 3.25 (m, 1H, H5''), 3.18 (m, 2H, H8''), 3.07 (m, 1H, H7''), 2.96 (m, 2H, H10, H7''), 2.82 (d, $J = 18.0$ Hz, 1H, H10), 2.57 (m, 1H, H5''), 2.33 (d, $J = 15.0$ Hz, 1H, H8), 2.12 (d, $J = 15.0$ Hz, 1H, H8), 1.98 (dd, $J = 12.5$, 12.5 Hz, 1H, H2''), 1.74 (d, $J = 12.5$ Hz, 1H, H2''), 1.27 (d, $J = 6.5$ Hz, 3H, H6''). ^{13}C NMR (150 MHz, CD_3OD , δ ppm): 214.72 (C13), 187.96 (C5), 187.60 (C12), 178.78 (C6''), 176.09 (C3''), 167.76 (C1''), 162.44 (C4), 157.33 (C6), 156.15 (C11), 137.26 (C2), 136.25 (C12a), 135.73 (C6a), 135.20 (C10a), 121.44 (C4a), 120.58 (C1), 120.36 (C3), 112.41 (C5a), 112.18 (C11a), 102.16 (C1''), 77.43 (C9), 71.27 (C7), 69.93 (C4''), 68.68 (C5''), 65.79 (C14), 57.21 (OCH₃), 47.63 (C3''), 41.91 (C2''), 41.36 (C4''), 40.15 (C8''), 37.32 (C8), 36.84 (C5''), 34.09 (C10), 30.61 (C2''), 30.06 (C7''), 17.36 (C6''). HRMS (ESI-TOF): calcd for $C_{35}H_{39}N_3O_{14}S$, 757.2153; found 757.2119 ($\Delta = 4.51$ ppm).

Synthesis of 13. To a solution of doxorubicin hydrochloride (113 mg, 194.83 μ mol, 1.5 equiv) in anhydrous DMF (5 mL), Et₃N (50 μ L, 363.69 μ mol, 2.8 equiv) was added and stirred for 30 min at room temperature. EMCS (48 mg, 155.87 μ mol, 1.2 equiv) was added and stirred further for 2 h at room temperature in a nitrogen atmosphere in the dark. Then, the solution was diluted 10 times in CH_2Cl_2 and filtered to remove the precipitated doxorubicin. The solution was concentrated and transferred into 10 volumes of diethyl ether to precipitate the product. The precipitate was collected by filtration and dried to obtain compound 2 as a red solid. The red solid was redissolved in anhydrous DMF (5 mL) and reacted with peptide 12 (89.9 mg, 129.89 μ mol, 1 eq; Peptron, Daejeon, South Korea) for 16 h at 4 °C in dark. The reaction was monitored using normal phase TLC ($CH_2Cl_2/MeOH/CH_3COOH$, 6:3:1, v/v/v). After the reaction was completed, the product was purified using a semipreparative HPLC system as mentioned above. The collected fraction of the product was lyophilized to obtain 13 as a red powder (136.9 mg, 73.8% yield). The purity was determined to be ≥95% by analytical HPLC. 1H NMR (800 MHz, DMSO-*d*₆, δ ppm): 8.73 (d, $J = 7.0$ Hz, 1H, 28''-N), 8.23 (d, $J = 7.5$ Hz, 2H, 14''-N, 23''-N), 8.16 (br s, 2H, 32''-N), 7.93 (m, 1H, 12''-N), 7.91 (m, 2H, H2, H3), 7.70 (d, $J = 7.9$ Hz, 1H, 18''-N), 7.65 (m, 1H, H1), 7.59 (br s, 1H, 35''-N), 7.48 (d, $J = 7.9$ Hz, 1H, 3'-N), 5.22 (d, $J = 3.0$ Hz, 1H, H1'), 4.95 (dd, $J = 4.5$, 4.5 Hz, 1H, H7), 4.61 (m, 1H, H28''), 4.57 (s, 2H, H14), 4.47 (dt, $J = 7.5$, 7.0 Hz, 1H, H14''), 4.28 (dt, $J = 7.5$, 7.0 Hz, 1H, H23''), 4.15 (q, $J = 6.5$ Hz, 1H, H5''), 4.11 (m, 1H, H18''), 3.98 (s, 3H, OCH₃), 3.95 (m, 2H, H3', H8''), 3.77 (m, 1H, H32''), 3.38 (s, 1H, H4''), 3.31 (dd, $J = 7.0$, 7.0 Hz, 2H, H6''), 3.23 (m, 2H, H12''), 3.14 (dd, $J = 7.0$, 14.0 Hz, 1H, H9''), 3.10 (m, 2H, H35''), 3.00 (d, $J = 16.5$ Hz, 1H, H10), 2.95 (d, $J = 16.5$ Hz, 1H, H10), 2.82 (m, 1H, H11''), 2.72 (m, 1H, H29''), 2.65 (m, 2H, H11'', H15''), 2.53 (m, 1H, H29''), 2.50 (m, 1H, H15''), 2.43 (m, 1H, H9''), 2.27 (ddd, $J = 5.5$, 11.0, 16.5 Hz, 1H, H25''), 2.21 (ddd, $J = 5.5$, 11.0, 16.5 Hz, 1H, H25''), 2.20 (m, 1H, H8), 2.12 (dd, $J = 4.5$, 14.0 Hz, 1H, H8), 2.02 (dd, $J = 7.0$, 7.0 Hz, 2H, H2''), 1.96 (m, 1H, H19''), 1.90 (m, 1H, H24''), 1.83 (ddd, $J = 3.0$, 12.0, 12.0 Hz, 1H, H2''), 1.73 (m, 1H, H24''), 1.72 (m, 2H, H33''), 1.54 (m, 2H, H34''), 1.41 (m, SH, H2', H3'', H5''), 1.15 (m, 2H, H4''), 1.12, (d, $J = 6.5$ Hz, 3H, H6''), 0.79–0.83 (m, 6H, H20'', H21''). HRMS (ESI-TOF): calcd for $C_{63}H_{85}N_{11}O_{25}S$, 1427.5439; found 1427.5433 ($\Delta = 0.39$ ppm).

Preparation of the Cyanine5.5-Labeled Prodrug. Cyanine5.5 NHS ester fluorescent dye was purchased from Lumiprobe (Hallandale Beach, FL) and was chemically labeled at the N-terminus of the DEVD moiety of 13. Compound 13 (5 mg, 3.5 μ mol) was dissolved in anhydrous DMF (0.2 mL), and Et₃N (1 μ L) was added. Cyanine5.5 NHS ester (3 mg, 4.2 μ mol) was added to the solution and reacted for 2 h at room temperature in nitrogen atmosphere in the dark. The reaction was monitored using normal phase TLC ($CH_2Cl_2/MeOH/CH_3COOH$, 6:3:1, v/v/v). After the reaction was completed, the solution was transferred into 10 volumes of CH_2Cl_2 and kept at

–20 °C overnight. The precipitate was collected by centrifugation and washed three times with cold CH₂Cl₂. The crude product was further purified with HPLC as mentioned above. The collected fraction of the product was lyophilized to obtain the final product as a dark greenish blue powder. The purity was determined to be ≥95% by analytical HPLC. ¹H NMR (800 MHz, DMSO-*d*₆, δ ppm): 8.45 (t, *J* = 13.0, 13.0 Hz, 2H, H22'', H24''), 8.25 (m, 2H, H14'', H34''), 8.20 (br s, 1H, 14''-N), 8.17 (br s, 1H, 28''-N), 8.11 (br s, 1H, 32''-N), 8.09 (d, *J* = 8.5 Hz, 1H, H29''), 8.07 (d, *J* = 8.5 Hz, 1H, H9''), 8.06 (m, 2H, H11'', H31''), 7.91 (m, 2H, H2, H3), 7.74 (d, *J* = 8.5 Hz, 1H, H28''), 7.71 (d, *J* = 8.5 Hz, 1H, H8''), 7.67 (m, 2H, H13'', H33''), 7.64 (m, 1H, H1), 7.51 (m, 2H, H12'', H32''), 7.48 (d, *J* = 8.0 Hz, 1H, 3'-N), 6.61 (t, *J* = 13.0 Hz, 1H, H23''), 6.35 (d, *J* = 13.5 Hz, 1H, H21''), 6.32 (d, *J* = 13.5 Hz, 1H, H25''), 5.22 (d, *J* = 3.5 Hz, 1H, H1'), 4.95 (dd, *J* = 4.3, 4.3 Hz, 1H, H7), 4.57 (s, 2H, H14), 4.51 (m, 1H, H28''), 4.45 (m, 1H, H14''), 4.21 (m, 4H, H23'', H32'', H6''), 4.15 (q, *J* = 6.5 Hz, 1H, H5''), 4.01 (m, 1H, H18''), 3.98 (s, 3H, OCH₃), 3.96 (m, 1H, H3''), 3.94 (m, 1H, H8''), 3.75 (s, 3H, H40''), 3.38 (s, 1H, H4''), 3.29 (t, *J* = 7.0 Hz, 2H, H6''), 3.23 (m, 2H, H12''), 3.13 (dd, *J* = 7.0, 14.0 Hz, 1H, H9''), 3.05 (t, *J* = 7.5 Hz, 2H, H35''), 2.99 (d, *J* = 16.5 Hz, 1H, H10), 2.95 (d, *J* = 16.5 Hz, 1H, H10), 2.83 (m, 1H, H11''), 2.70 (m, 1H, H29''), 2.66 (m, 1H, H11''), 2.52 (m, 2H, H15''), 2.49 (m, 1H, H29''), 2.41 (m, 1H, H9''), 2.19 (m, 3H, H8, H25''), 2.14 (m, 3H, H8, H2'''), 2.01 (dd, *J* = 7.0, 7.0 Hz, 2H, H2''), 1.97–1.95 (m, 1H, H24'', H19'', H20'', H38'', H39''), 1.94 (m, 1H, H19''), 1.82 (ddd, *J* = 3.5, 13.0, 13.0 Hz, 1H, H2''), 1.76 (m, 1H, H24''), 1.74 (m, 2H, H5''), 1.63 (m, 1H, H33''), 1.56 (m, 2H, H3''), 1.47 (m, 3H, H33'', H34''), 1.42 (m, 1H, H2''), 1.40 (m, 6H, H3'', H5'', H4''), 1.14 (m, 2H, H4''), 1.11 (d, *J* = 6.5 Hz, 3H, H6''), 0.78–0.82 (m, 6H, H20'', H21''). HRMS (ESI-TOF): calcd for C₁₀₃H₁₂₆N₁₃O₂₆S, 1992.8658; found 1992.8684 (Δ = 1.32 ppm).

In Vitro MTT Cytotoxicity Assay. The MTT assay kit was purchased from Trevigen (Gaithersburg, MD). High glucose Dulbecco's modified Eagle's medium (DMEM), phosphate buffered saline (PBS), and fetal bovine serum (FBS) were from Gibco (Carlsbad, CA). MDA-MB-231 cells were obtained from American Type Culture Collection (ATCC, Manassas, VA). The assay was carried out using the standard procedures to evaluate the cytotoxicity of the synthesized products. Briefly, MDA-MB-231 cells were grown in DMEM supplemented with 10% FBS, harvested, and plated at a density of 5 × 10⁴ cell per well in 96 well culture plates (Corning, Tewksbury, MA). After 24 h of incubation, doxorubicin, 6, 7, 8, 9, 10, and 11 were treated at concentrations of 0.1, 1, 10, and 100 μM with the cells and further incubated for 48 h. The medium was replaced with 100 μL prewarmed PBS, and 10 μL of MTT reagent was added and incubated for 2 h at 37 °C, subsequently. When purple formazan precipitates were observed clearly in the cells, 100 μL of detergent agent was further added and incubated for 4 h at room temperature. After the precipitates were clearly solubilized, absorbance was measured at 570 nm using a microplate reader (Synergy HT; BioTek Instruments, Winooski, VT).

In Vitro MTT Cytotoxicity Assay of Prodrug 13 Coupled with Radiation. MDA-MB-231 cells were grown in 96 well culture plates. Prodrug 13 was treated at 5 μM, and the cells were exposed to 5 Gy of linear X-ray. The cells were incubated for 24 and 48 h, and the cytotoxicity was determined by the standard MTT cytotoxicity assay procedure as described above.

In Vitro Cellular Uptake Imaging. Intracellular distribution of doxorubicin, 6, 7, 8, 9, 10, and 11 was observed under confocal laser scanning microscopy. MDA-MB-231 cells were seeded on 35 mm cover glass-bottomed dishes (SPL Life Sciences, Pocheon, Korea) at a density of 5 × 10⁵ cells per dish and allowed to grow overnight. The synthesized doxorubicin derivatives or doxorubicin were treated with the cells at 10 μM final concentration and further incubated for 18 h. The cells were washed with cold PBS and fixed with 4% paraformaldehyde (Sigma-Aldrich). The nucleus was stained using DAPI (Molecular Probes, Eugene, OR) and observed under confocal laser scanning microscopy (LSM 710; Carl Zeiss, Oberkochen, Germany). The mean pixel intensity of the accumulated compound

in the nuclei was quantitatively determined using ImageJ software (National Institutes of Health, Bethesda, MD).

In Vitro Cellular Uptake Imaging of Prodrug 13 Coupled with Radiation. MDA-MB-231 cells were grown as described above and incubated with prodrug 13 (5 μM) for 24 h. Then the cells were exposed to 5 Gy of linear X-ray and further incubated for 6 or 24 h. The cells were washed with PBS, fixed with 4% paraformaldehyde, and stained with DAPI. The cellular uptake and distribution of prodrug 13 was observed under focus drift compensating fluorescent microscopy (IX81-ZDC, Olympus, Tokyo, Japan) at 470/580 nm.

Determination of the Octanol–Water Partition Coefficient. The partition coefficient of compounds 7, 8, 9, 10, and 11 was determined by using the shake-flask method. Each compound (100 μg) was dissolved (or suspended) in 200 μL of *n*-octanol, and then an equal volume of distilled water was added. The tube was vigorously vortexed for 3 h to allow the compound to partition to each phase. The organic and aqueous phases were allowed to separate, and the concentration of the compound in each phase was measured by fluorescent spectroscopy with standard solutions. The experiment was done in triplicate. The partition coefficient of the tested compounds was calculated according to the following equation:

$$\log P = \log \left(\frac{[\text{compound}]_{\text{organic}}}{[\text{compound}]_{\text{aqueous}}} \right)$$

In Vitro Caspase-Mediated Activation Assay. To determine the activation of prodrug 13 by caspase-3, the prodrug (100 μM) was incubated with recombinant human caspase-3 (500 ng/mL; R&D Systems, Minneapolis, MN) in the caspase assay buffer (50 mM HEPES, pH 7.4, 100 mM NaCl, 0.1% CHAPS, 10 mM DTT, 1 mM EDTA, and 10% glycerol; Enzo Life Sciences, Farmingdale, NY) at room temperature. Small portion of the solution was withdrawn at 15, 30, and 60 min time points, and the reaction were quenched by the addition of equal volumes of DMSO. The withdrawn samples were subjected to analytical HPLC (Agilent 1300 series, Agilent Technologies) using an ODS-A 5 μm analytical column (150 mm × 3 mm; YMC, Dinslaken, Germany). A gradient system (water and CH₃CN with 0.1% TFA as an additive, CH₃CN 20–30%/5–25 min) was applied at a flow rate of 0.8 mL/min. The chromatogram was monitored under a fluorescence detector at 470/580 nm. The ratio of remaining prodrug 13 and released compound 8 was determined based on the area of the peaks. Additionally, prodrug 13 without caspase-3 and also with recombinant human caspase-3 (500 ng/mL) pretreated with Ac-DEVD-CHO (10 μM; Enzo Life Sciences) were incubated for 60 min at room temperature in the caspase assay buffer and subjected to analytical HPLC.

In Vitro Caspase-Mediated Activation and Cellular Uptake Imaging. Intracellular distribution of Cyanine5.5-labeled prodrug 13 was observed to assess the intracellular distribution with or without caspase-3. MDA-MB-231 cells were seeded on 35 mm covered glass-bottomed dishes as described above. The Cyanine5.5-labeled prodrug 13 was treated with the cells at a final concentration of 100 μM and incubated for 1 h in the absence of recombinant human caspase-3 (500 ng/mL). The cells were washed with cold PBS and fixed with 4% paraformaldehyde. Then, the cells were stained with DAPI and observed under confocal laser scanning microscopy (LSM 710; Carl Zeiss). The fluorescent signal of Cyanine5.5 was presented in green as a pseudocolor, and the red fluorescence was enhanced using ZEN 2013 software (Carl Zeiss).

Western Blot. MDA-MB-231 cells were irradiated in plates with a 6-MV photon beam generated by a linear accelerator (Varian Co, Milpitas, CA), which delivers a dose rate of 4 Gy/min. After 24, 48, or 72 h, the cells were lysed and subjected to Western blotting according to the standard protocol. For immunoblotting, anti-procaspase-3 antibody (1:1000; Abcam, Cambridge, MA), anti-active (cleaved) caspase-3 antibody (1:1000; abcam), and anti-β-actin antibody (Sigma-Aldrich) were used as primary antibodies. HRP-conjugated anti-rabbit or anti-mouse IgG antibody (1:2000; Zymed, San Francisco, CA) was used as the secondary antibody. The blotted membranes were developed using a Supersignal West Pico

Chemiluminescent substrate (Pierce Biotechnology, Rockford, IL) following the manufacturer's protocol.

For another set of experiments, the cells were treated with 1, 10, and 100 μM compound **8** or prodrug **13** and incubated for 48 h. For immunoblotting, anti-procaspase-3 antibody (1:1000; Cell Signaling Technology, Danvers, MA), anti-active caspase-3 antibody (1:1000; Cell Signaling Technology), and anti- β -actin antibody (Sigma-Aldrich) were used as primary antibodies. HRP-conjugated anti-rabbit or anti-mouse IgG antibody (1:2000; R&D Systems) was used as the secondary antibody. The blotted membranes were incubated with luminol reagent (Santa Cruz Biotechnology, Dallas, TX) and developed using an ImageQuant LAS 4000 imaging system (GE Healthcare Life Sciences, Uppsala, Sweden).

Animal Experiment. All experimental procedures were approved by the Institutional Animal Care and Use Committee of Seoul National University. The murine squamous cell carcinoma (SCC7; Korean Cell Line Bank, Seoul, Korea) was cultured in DMEM supplemented with 10% FBS, harvested, and resuspended at 1×10^7 cell/mL. The cell suspension (100 μL) was inoculated subcutaneously into the thigh of 6 week-old male C3H/HeN mice. When the tumor volume reached 50–100 mm³, the tumor-bearing mice were randomized ($n = 5$). The treatment group received prodrug **13** for 7 days daily at a dose of 14 mg/kg (equivalent to 5 mg/kg of doxorubicin) via tail vein intravenous administration. For radiation-treated groups, 10 Gy of X-ray (6 MV, 300 cGy/min; Clinac 21EX, Varian, Palo Alto, CA) was given once to the tumor at the first day of drug treatment. The control group received normal saline for 7 days daily. The tumor length and width were measured by calipers, and the volume was calculated using the modified ellipsoid formula (length \times width²/2).

Statistical Analysis. Data are presented as the means \pm SEM. The differences between groups were determined by the Mann–Whitney *U* test. GraphPad Prism, version 6.0 (GraphPad Software, San Diego, CA) software was used for the statistical calculations. All statistical tests were one-tailed, and *P* values less than 0.05 were considered significant.

■ ASSOCIATED CONTENT

Supporting Information

The Supporting Information is available free of charge on the ACS Publications website at DOI: [10.1021/acs.jmedchem.5b00420](https://doi.org/10.1021/acs.jmedchem.5b00420).

Whole-set of images of the confocal microscopic images and full-length blots of the Western blot results, survival rate of animals administered with prodrug **13** or doxorubicin, ¹H and ¹³C NMR spectra, and HPLC chromatograms of the purified compounds ([PDF](#))

■ AUTHOR INFORMATION

Corresponding Authors

*(S.Y.K.) Phone: 82-2-3010-3715. Fax: 82-2-489-2773. E-mail: sykim2@amc.seoul.kr.

*(Y.B.) Phone: 82-2-880-7866. Fax: 82-2-872-7864. E-mail: yrbyun@snu.ac.kr.

Notes

The authors declare no competing financial interest.

■ ACKNOWLEDGMENTS

This study was supported by grants from the Bio & Medical Technology Development Program (grant no. 2012028833) and Basic Science Research Program (grant no. 2010-0027955) through the National Research Foundation of Korea (NRF) funded by the Korea government [MSIP]. We also thank Tae Hyung Won (Natural Products Research Institute, College of

Pharmacy, Seoul National University) for his great support in characterization of the synthesized compounds.

■ ABBREVIATIONS USED

AMAS, *N*-(α -maleimidocaproyloxy)succinimide ester; CASP3, caspase-3; CHAPS, 3-[3-cholamidopropyl]-dimethylammonio]-1-propanesulfonate; DAPI, 4',6-diamidino-2-phenylindole; DMEM, Dulbecco's modified Eagle's medium; DMF, dimethylformamide; DMSO, dimethyl sulfoxide; DNA, deoxyribonucleic acid; DTT, dithiothreitol; DXR, doxorubicin; EDTA, ethylenediaminetetraacetic acid; EMCS, *N*-(ϵ -maleimidocaproyloxy)succinimide ester; ESI-TOF, electrospray ionization time-of-flight mass spectrometry; FBS, fetal bovine serum; Gy, gray; HEPES, 4-(2-hydroxyethyl)piperazine-1-ethanesulfonic acid; HPLC, high performance liquid chromatography; HRMS, high resolution mass spectrometry; HRP, horseradish peroxidase; i.v., intravenous; MBS, *m*-maleimidobenzoyl-N-hydroxysuccinimide ester; MTT, methylthiazol tetrazolium; NHS, *N*-hydroxysuccinimide; NMR, nuclear magnetic resonance; ODS, octadecyl silica; PABC, *p*-aminobenzyloxycarbamate; PBS, phosphate buffered saline; RIPA, radioimmunoprecipitation assay; SCC, squamous cell carcinoma; SMCC, succinimidyl 4-(*N*-maleimidomethyl)cyclohexane-1-carboxylate; SMPB, succinimidyl 4-(*p*-maleimidophenyl)-butyrate; TFA, trifluoroacetic acid; TLC, thin layer chromatography; UV, ultraviolet

■ REFERENCES

- (1) Krüger, M.; Beyer, U.; Schumacher, P.; Unger, C.; Zahn, H.; Kratz, F. Synthesis and stability of four maleimide derivatives of the anticancer drug doxorubicin for the preparation of chemoimmunoconjugates. *Chem. Pharm. Bull.* **1997**, *45*, 399–401.
- (2) Zhang, S.; Liu, X.; Bawa-Khalfe, T.; Lu, L. S.; Lyu, Y. L.; Liu, L. F.; Yeh, E. T. Identification of the molecular basis of doxorubicin-induced cardiotoxicity. *Nat. Med.* **2012**, *18*, 1639–1642.
- (3) Assumpção, J. U.; Campos, M. L.; Ferraz Nogueira Filho, M. A.; Pestana, K. C.; Baldan, H. M.; Formariz Pilon, T. P.; de Oliveira, A. G.; Peccinini, R. G. Biocompatible microemulsion modifies the pharmacokinetic profile and cardiotoxicity of doxorubicin. *J. Pharm. Sci.* **2013**, *102*, 289–296.
- (4) DiPaola, R. S.; Rinehart, J.; Nemunaitis, J.; Ebbinghaus, S.; Rubin, E.; Capanna, T.; Ciardella, M.; Doyle-Lindrud, S.; Goodwin, S.; Fontaine, M.; Adams, N.; Williams, A.; Schwartz, M.; Winchell, G.; Wickersham, K.; Deutsch, P.; Yao, S. L. Characterization of a novel prostate-specific antigen-activated peptide-doxorubicin conjugate in patients with prostate cancer. *J. Clin. Oncol.* **2002**, *20*, 1874–1879.
- (5) Sapra, P.; Stein, R.; Pickett, J.; Qu, Z.; Govindan, S. V.; Cardillo, T. M.; Hansen, H. J.; Horak, I. D.; Griffiths, G. L.; Goldenberg, D. M. Anti-CD74 antibody-doxorubicin conjugate, IMMU-110, in a human multiple myeloma xenograft and in monkeys. *Clin. Cancer Res.* **2005**, *11*, 5257–5264.
- (6) Rypa, C.; Mann-Steinberg, H.; Fichtner, I.; Weber, H.; Satchi-Fainaro, R.; Binioksek, M. L.; Kratz, F. In vitro and in vivo evaluation of doxorubicin conjugates with the divalent peptide E-[c(RGDfK)2] that targets integrin alphavbeta3. *Bioconjugate Chem.* **2008**, *19*, 1414–1422.
- (7) Ai, S.; Duan, J.; Liu, X.; Bock, S.; Tian, Y.; Huang, Z. Biological evaluation of a novel doxorubicin-peptide conjugate for targeted delivery to EGF receptor-overexpressing tumor cells. *Mol. Pharmaceutics* **2011**, *8*, 375–386.
- (8) Saha, P.; Fortin, S.; Leblanc, V.; Parent, S.; Asselin, E.; Berube, G. Design, synthesis, cytoidal activity and estrogen receptor alpha affinity of doxorubicin conjugates at 16alpha-position of estrogen for site-specific treatment of estrogen receptor positive breast cancer. *Steroids* **2012**, *77*, 1113–1122.

- (9) Swanton, C. Intratumor heterogeneity: evolution through space and time. *Cancer Res.* **2012**, *72*, 4875–4882.
- (10) Marusyk, A.; Almendro, V.; Polyak, K. Intra-tumour heterogeneity: a looking glass for cancer? *Nat. Rev. Cancer* **2012**, *12*, 323–334.
- (11) Bae, Y. H. Drug targeting and tumor heterogeneity. *J. Controlled Release* **2009**, *133*, 2–3.
- (12) Gerlinger, M.; Rowan, A. J.; Horswell, S.; Larkin, J.; Endesfelder, D.; Gronroos, E.; Martinez, P.; Matthews, N.; Stewart, A.; Tarpey, P.; Varela, I.; Phillimore, B.; Begum, S.; McDonald, N. Q.; Butler, A.; Jones, D.; Raine, K.; Latimer, C.; Santos, C. R.; Nohadani, M.; Eklund, A. C.; Spencer-Dene, B.; Clark, G.; Pickering, L.; Stamp, G.; Gore, M.; Szallasi, Z.; Downward, J.; Futreal, P. A.; Swanton, C. Intratumor heterogeneity and branched evolution revealed by multiregion sequencing. *N. Engl. J. Med.* **2012**, *366*, 883–892.
- (13) Bae, Y. H.; Park, K. Targeted drug delivery to tumors: myths, reality and possibility. *J. Controlled Release* **2011**, *153*, 198–205.
- (14) Cho, Y. W.; Kim, S. Y.; Kwon, I. C.; Kim, I. S. Complex adaptive therapeutic strategy (CATS) for cancer. *J. Controlled Release* **2014**, *175*, 43–47.
- (15) Lee, B. S.; Cho, Y. W.; Kim, G. C.; Lee do, H.; Kim, C. J.; Kil, H. S.; Chi, D. Y.; Byun, Y.; Yuk, S. H.; Kim, K.; Kim, I. S.; Kwon, I. C.; Kim, S. Y. Induced phenotype targeted therapy: radiation-induced apoptosis-targeted chemotherapy. *J. Natl. Cancer Inst.* **2015**, *107*, dju403.10.1093/jnci/dju403
- (16) Agnieszamy, J.; Fang, B.; Weber, I. T. Plasticity of S2-S4 specificity pockets of executioner caspase-7 revealed by structural and kinetic analysis. *FEBS J.* **2007**, *274*, 4752–4765.
- (17) Asakura, T.; Sawai, T.; Hashidume, Y.; Ohkawa, Y.; Yokoyama, S.; Ohkawa, K. Caspase-3 activation during apoptosis caused by glutathione-doxorubicin conjugate. *Br. J. Cancer* **1999**, *80*, 711–715.
- (18) Ueno, M.; Kakinuma, Y.; Yuhki, K.; Murakoshi, N.; Iemitsu, M.; Miyauchi, T.; Yamaguchi, I. Doxorubicin induces apoptosis by activation of caspase-3 in cultured cardiomyocytes in vitro and rat cardiac ventricles in vivo. *J. Pharmacol. Sci.* **2006**, *101*, 151–158.
- (19) Thornberry, N. A.; Rano, T. A.; Peterson, E. P.; Rasper, D. M.; Timkey, T.; Garcia-Calvo, M.; Houtzager, V. M.; Nordstrom, P. A.; Roy, S.; Vaillancourt, J. P.; Chapman, K. T.; Nicholson, D. W. A combinatorial approach defines specificities of members of the caspase family and granzyme B. Functional relationships established for key mediators of apoptosis. *J. Biol. Chem.* **1997**, *272*, 17907–17911.
- (20) Yoshimori, A.; Takasawa, R.; Tanuma, S. A novel method for evaluation and screening of caspase inhibitory peptides by the amino acid positional fitness score. *BMC Pharmacol.* **2004**, *4*, 7.
- (21) Lien, S.; Pastor, R.; Sutherlin, D.; Lowman, H. B. A substrate-phage approach for investigating caspase specificity. *Protein J.* **2004**, *23*, 413–425.
- (22) Stennicke, H. R.; Salvesen, G. S. Caspase assays. *Methods Enzymol.* **2000**, *322*, 91–100.
- (23) Dubowchik, G. M.; Firestone, R. A.; Padilla, L.; Willner, D.; Hofstead, S. J.; Mosure, K.; Knipe, J. O.; Lasch, S. J.; Trail, P. A. Cathepsin B-labile dipeptide linkers for lysosomal release of doxorubicin from internalizing immunoconjugates: model studies of enzymatic drug release and antigen-specific in vitro anticancer activity. *Bioconjugate Chem.* **2002**, *13*, 855–869.
- (24) Chen, Q.; Sowa, D. A.; Cai, J.; Gabathuler, R. Efficient one-pot synthesis of doxorubicin conjugates through its amino group to melanotransferrin P97. *Synth. Commun.* **2003**, *33*, 2401–2421.
- (25) Chen, Q.; Sowa, D. A.; Cai, J.; Gabathuler, R. Synthesis of doxorubicin conjugates through hydrazone bonds to melanotransferrin P97. *Synth. Commun.* **2003**, *33*, 2377–2390.
- (26) Garsky, V. M.; Lumma, P. K.; Feng, D. M.; Wai, J.; Ramjit, H. G.; Sardana, M. K.; Oliff, A.; Jones, R. E.; DeFeo-Jones, D.; Freidinger, R. M. The synthesis of a prodrug of doxorubicin designed to provide reduced systemic toxicity and greater target efficacy. *J. Med. Chem.* **2001**, *44*, 4216–4224.
- (27) Jain, M.; Barthwal, S. K.; Barthwal, R.; Govil, G. Restrained molecular dynamics studies on complex of adriamycin with DNA hexamer sequence d-CGATCG. *Arch. Biochem. Biophys.* **2005**, *439*, 12–24.
- (28) Huang, Q.; Li, F.; Liu, X.; Li, W.; Shi, W.; Liu, F. F.; O'Sullivan, B.; He, Z.; Peng, Y.; Tan, A. C.; Zhou, L.; Shen, J.; Han, G.; Wang, X. J.; Thorburn, J.; Thorburn, A.; Jimeno, A.; Raben, D.; Bedford, J. S.; Li, C. Y. Caspase 3-mediated stimulation of tumor cell repopulation during cancer radiotherapy. *Nat. Med.* **2011**, *17*, 860–866.